REPORT DOCUMENTATION PAGE

Form Approved
OMB No. 0704-0188

1. REPORT DATE *(DD-MM-YYYY)*	2. REPORT TYPE	3. DATES COVERED *(From - To)*
	Technical Paper	

4. TITLE AND SUBTITLE

5a. CONTRACT NUMBER
F04611-01-C-0010

5b. GRANT NUMBER

5c. PROGRAM ELEMENT NUMBER

6. AUTHOR(S)

5d. PROJECT NUMBER
BMDO

5e. TASK NUMBER
SBRU

5f. WORK UNIT NUMBER

7. PERFORMING ORGANIZATION NAME(S) AND ADDRESS(ES)

8. PERFORMING ORGANIZATION REPORT

9. SPONSORING / MONITORING AGENCY NAME(S) AND ADDRESS(ES)

Air Force Research Laboratory (AFMC)
AFRL/PRS
5 Pollux Drive
Edwards AFB CA 93524-7048

10. SPONSOR/MONITOR'S ACRONYM(S)

11. SPONSOR/MONITOR'S NUMBER(S)

12. DISTRIBUTION / AVAILABILITY STATEMENT

Approved for public release; distribution unlimited.

13. SUPPLEMENTARY NOTES

14. ABSTRACT

15. SUBJECT TERMS

16. SECURITY CLASSIFICATION OF:			17. LIMITATION OF ABSTRACT	18. NUMBER OF PAGES	19a. NAME OF RESPONSIBLE PERSON
a. REPORT	b. ABSTRACT	c. THIS PAGE			Leilani Richardson
Unclassified	Unclassified	Unclassified	A		19b. TELEPHONE NUMBER *(include area code)* (661) 275-5015

Standard Form 298 (Rev. 8-98)
Prescribed by ANSI Std. 239.18

4 separate items are enclosed

1119 1 of 20

BADOSBRU DTSV

MEMORANDUM FOR PRS (Contractor Publication) 01 C 8010

FROM: PROI (STINFO) 22 March 2002

SUBJECT: Authorization for Release of Technical Information, Control Number: **AFRL-PR-ED-TP-2002-066**
Gary Cheng (UAB); Curtis Johnson (Sierra); Richard Cohn (PRSA), "Swirl Coaxial Injector Development Part II CFD Modeling"

Rich 56177

JANNAF Joint Propulsion Meeting **(Statement A)**
(Destin, FL, 8-12 April 2002) **(Deadline: 08 April 02)**

SWIRL COAXIAL INJECTOR DEVELOPMENT
PART II CFD MODELING

G. C. Cheng, ME Dept., UAB
C. W. Johnson and J. A. Muss, Sierra Engineering Inc.
R. K. Cohn, Air Force Research Laboratory, Edwards AFB, CA

ABSTRACT

Injector design is critical to obtaining the dual goals of long engine life as well as providing high energy release efficiency in the main combustion chamber. Introducing a swirl component in the injector flow can enhance the propellant mixing and thus improve engine performance. A combined experimental and computational effort is underway to examine the properties of GOX-centered, swirl coaxial injectors to examine their performance and lifetime characteristics. These injectors can be easily manufactured and can be designed to maintain a low face temperature, which will improve engine life. Therefore, swirl coaxial injectors, which swirl liquid fuel around a gaseous oxygen core, show promise for the next generation of high performance staged combustion rocket engines utilizing hydrocarbon fuels. The purpose of this work is to not only examine the properties of these injectors, but also to develop a design methodology, utilizing a combination of high-pressure cold-flow testing, uni-element hot-fire testing, and computations to create a high performing, long life swirl coaxial injector for multi-element combustor use. Several swirl coax injector configurations designed and fabricated by Sierra Engineering have been tested at the Edwards AFB Research site of the Air Force Research Laboratory Propulsion Directorate. An integral part of this effort is the use of computational fluid dynamics (CFD) analyses to both gain insight into the flowfield to improve our understanding of the underlying flow characteristics of this injector, as well as to help determine the ability of CFD to provide this. Both cold-flow and hot-fire analyses were completed, but only the cold flow results are presented and discussed in this paper. The FDNS-RFV CFD code was employed, with the homogeneous real-fluid model selected to simulate the spray combustion phenomena for both the cold flow and hot fire conditions. Initial results show that large-scale phenomenology was predicted well by the cold-flow CFD analysis. Analyses and test comparisons will be presented and an assessment of the utility of the analyses will be discussed. More details of the experimental results can be found in the Part I companion paper (1).

INTRODUCTION

Sierra Engineering and the Air Force Research Laboratory (AFRL) have undertaken a program to develop a swirl coaxial injector. The element will be used in an Alternate Fuels Testbed (AFT) combustor to test hydrocarbon fuel performance and operability. To produce meaningful results, the 2000 lbf thrust, 1500 psi chamber pressure, multi-element combustor must be high performing and adaptable to different hydrocarbon based fuels. The combustor will operate on ambient temperature gaseous oxygen and an array of fuels. In order to facilitate the testing of a variety of fuels, the combustor is designed with removable injector elements, allowing tailored elements if it proves necessary.

The injector development program started with 11 candidate single element designs, each was first cold flow tested in the high pressure injector characterization facility at AFRL. These same elements are now undergoing an extensive hot fire test sequence in AFRL's EC-1 facility. The final phase of this program will be the testing of the multi-element AFT combustor at AFRL's 1-14 test facility. See part 1[1] for complete information on the hardware design and test results.

In coordination with the testing, a CFD analysis effort has been undertaken to predict injector performance, and more importantly, to gain insight into the physics and the trends for different designs of the swirl coaxial elements. Both cold flow uni-element analyses and hot fire uni-element analyses have been completed. This paper discusses the CFD solutions of the cold flow tests and compares these solutions to the test data.

The Single-Wall Swirl Coaxial element

Figure 1 shows a cut-away of the simple, single wall swirl coaxial element. Gaseous oxidizer flows through the center of the element (GOX post). No swirl component is given to the oxidizer. The fuel is injected tangentially at three or four symmetrically located ports around the GOX post wall. The fuel then swirls around the GOX post wall, creating a sheet, which becomes entrained in the oxidizer and swept out of the element. Figure 1 shows a GOX post with a divergent cone at the tip. Several different geometries have been fabricated and tested for this section of the element.

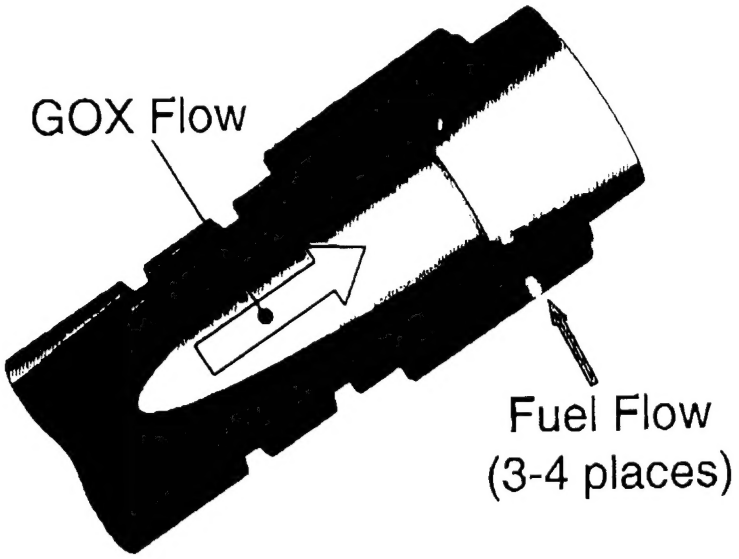

Figure 1. Coaxial Element cut-away.

NUMERICAL MODELS

The present study employed a finite difference Navier-Stokes (FDNS) CFD flow solver[1-6] to analyze the liquid swirl injectors. The real-fluid submodel was incorporated into the FDNS solver (FDNS-RFV) to simulate liquid spray phenomena. The FDNS code has been widely employed by NASA MSFC to analyze various flow problems of rocket engines. The framework of the FDNS-RFV code is an elliptic finite difference Navier-Stokes flow solver employing a predictor plus a multi-corrector pressure-based solution algorithm. Higher order upwind, total variation diminishing (TVD), or central difference schemes plus adaptive second-order and fourth-order dissipation terms are used to approximate the convection terms of the transport equations. Various matrix solvers, such as vectorized point implicit, conjugate gradient, and generalized minimal residual[9] (GMRES), are provided in the code so that users can select one for a given transport equation. Since the FDNS-RFV flow solver is a structured code, multi-block, multi-zone options are included so that problems with complex geometries can be analyzed efficiently. For the homogeneous spray model, the sound speed of a multi-component mixture must be calculated from the real-fluid property submodel to properly account for the compressibility effect.

The proposed homogeneous spray model has been used to simulate a single element like-on-like (LOL) impinger injector element and a single element unlike impinger element for the configuration and flow conditions used in the cold-flow experiments. The numerical results were shown to agree fairly well with the analytical model[3]. Recently, the proposed homogeneous spray model was employed to simulate cryogenic nitrogen injections and spray combustion of GH_2/LO_2 shear coaxial injectors. The comparisons of the numerical results with the test data were successful[1]. Hence, the homogeneous spray model was utilized to analyze the swirl injectors. Note that

this model assumes that the particulate phase and the gas phase to be in equilibrium and is most suitable for mixing at super and near critical conditions. The cold flow tests utilize sub-critical water injection, which may lead to some inaccuracies.

Since the cold flow tests were conducted under subcritical conditions, and the homogenous spray model is better suited for supercritical conditions, one must be careful in the interpretation of the results. Under supercritical conditions, droplets do not exist. However, it is believed that droplet sizes measured under subcritical conditions correspond to the size of structural features found in supercritical conditions. Thus, smaller drop sizes in the subcritical conditions will correspond to smaller structural length scales under supercritical conditions. It is also likely that the mass flux distribution pattern measured in the subcritical, cold flow tests will, in theory, have a smaller spatial distribution, i.e., there will be less smearing, than would under supercritical conditions. Similar results have been seen in Chehroudi *et al.*[11] where it was found that the spreading rate of a supercritical jet is significantly larger than that for subcritical jets. The increased spreading rate, combined with the lack of a latent heat of vaporization in the supercritical condition will likely yield an increase in mixing over the subcritical case.

Three swirl injector configurations (Injector #4, #7, and #11 shown in Figure 2) and two operating conditions (chamber pressure P_c = 271 psig, and 842 psig) were simulated in this numerical study. Studying different injector configurations helped analyze the effect of geometry on the propellant mixing, while investigating different operating conditions reveals the trend of the propellant mixing with chamber pressure. The numerical results for various cases were compared to the test data, and are reported herein.

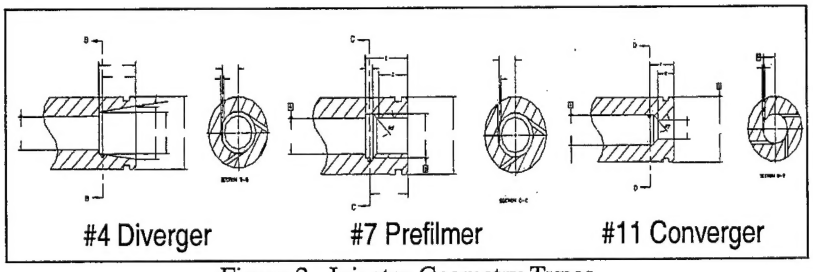

Figure 2. Injector Geometry Types

The operating condition, boundary conditions, and injector geometry in a typical numerical simulation are illustrated in Figure 3. As Figure 3 shows, an entrain boundary condition simulated the cavity region outside of the injector faceplate. The injectors with three fuel injector holes were spaced at 120°, while the injector with four fuel injection holes used a 90° pie section. A two-zone mesh system was constructed to represent the whole computational domain. The injector section designated as the first zone consists of approximately a 45x31x43 grid system; while the second zone, approximately a 71x101x43 mesh system, was employed to model the chamber section. Exact grid dimensions depended on the geometry.

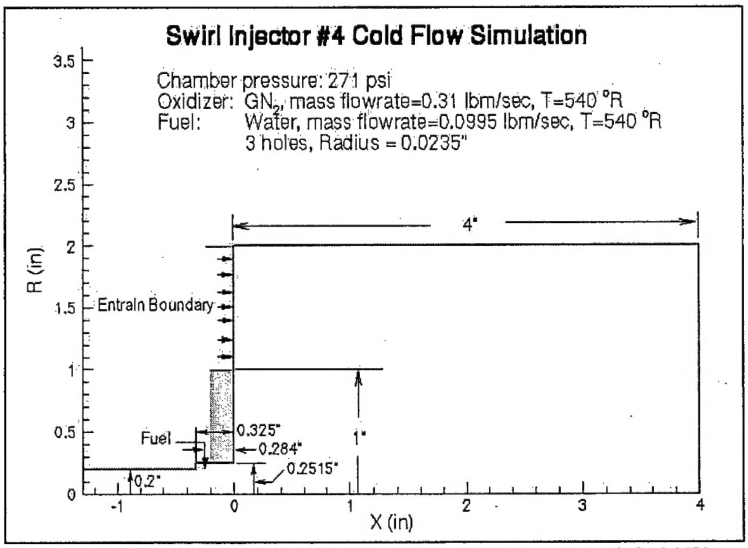

Figure 3. The Flow and Boundary Conditions of a Typical Numerical Cold Flow Simulation

RESULTS

CFD solutions for the cold flow simulations are presented in this section. Discussion of the results follows. Results will be presented for injector #4 followed by #7 and #11. Simulation results for injector #4 are shown in Figures 4-9. Figure 4 shows fuel (water) mass fraction at various circumferential planes while Figure 5 shows fuel mass flux at various axial planes. Figures 6 and 7 show streamlines of fuel and GOX (gaseous N_2) respectively. Figure 8 shows how the mass flux fans out as the spray leaves the injector. The predicted fuel mass fluxes at two inches downstream from the injector exit are compared to the test data and illustrated in Figure 9. It is obvious that there is a discrepancy in the absolute value of the mass flux between the numerical result and the test data. This discrepancy is likely caused by the large amount of the test water flow not measured in the patternator. As described in part I, the loss of fluid is the result of a stagnation region that is generated near the entrance of the patternator tubes. This region prevents some of the smaller droplets from entering the tube. Comparing the amount of water entering the facility with the amount measured in the patternator, it was found that the collection efficiency was significantly less then 100% (ranging from 22%-65% for the experiments conducted). In order to account for the lost fluid, the mass flux is scaled to account for the lost mass. However, the stagnation region will be stronger near the centerline and could result in a disproportionate amount of fluid being lost in that region as well as the ability to discern features of the max flux distrubution.

Figures 10-15 and 16-21 display similar simulation results for injectors 7 and 11 respectively. Comparing the three injectors, it is interesting to note that in the pre-filmer design (#7) and the converging design (#11), most of the asymmetries in the mixing field are removed by x = 2". However, the diverging design (#4) maintains the asymmetrical pattern to x = 4". This could result in uneven heat release in the engine chamber if these trends persist in the hot-fire data.

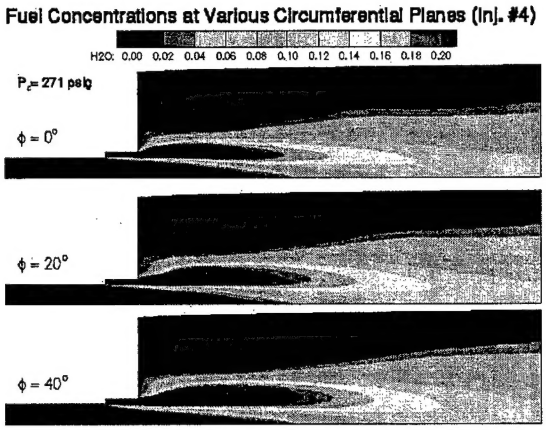

Figure 4. Mass Fraction Contours of Fuel at Various Circumferential Planes (Injector #4)

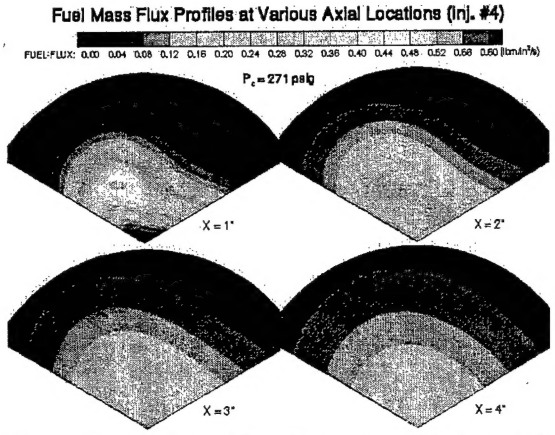

Figure 5. Fuel Mass Flux Contours at Various Axial Locations

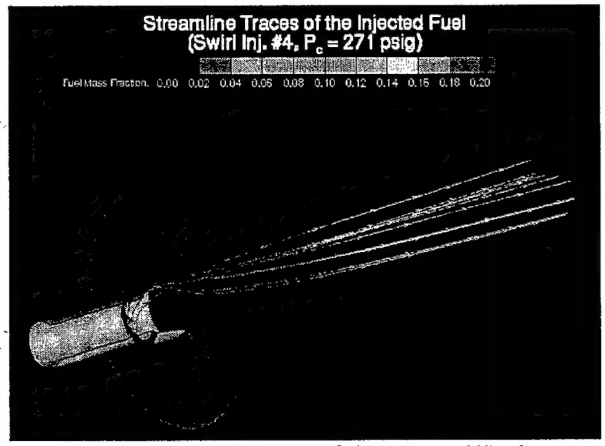

Figure 6. Streamline Traces of the Injected Fuel

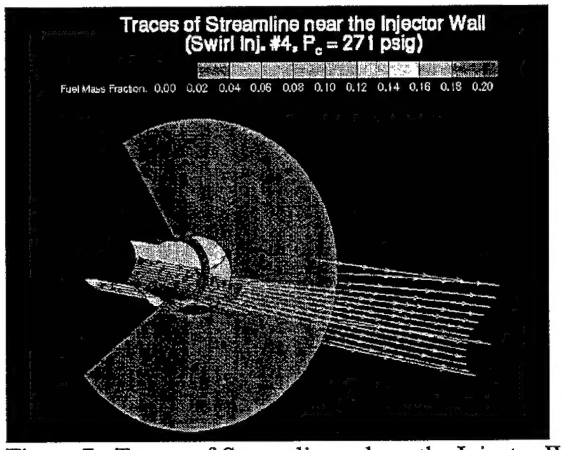

Figure 7. Traces of Streamlines along the Injector Wall

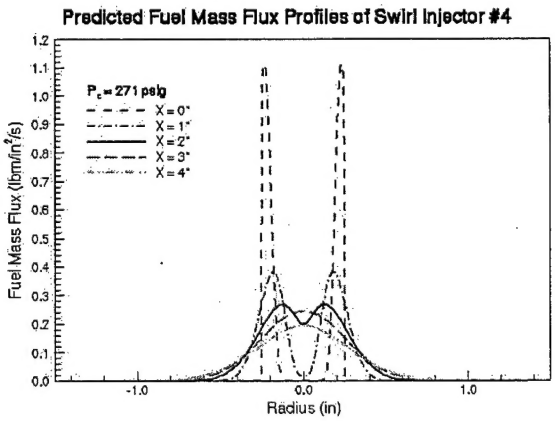

Figure 8. Averaged Mass Flux of Fuel at Various Axial Locations

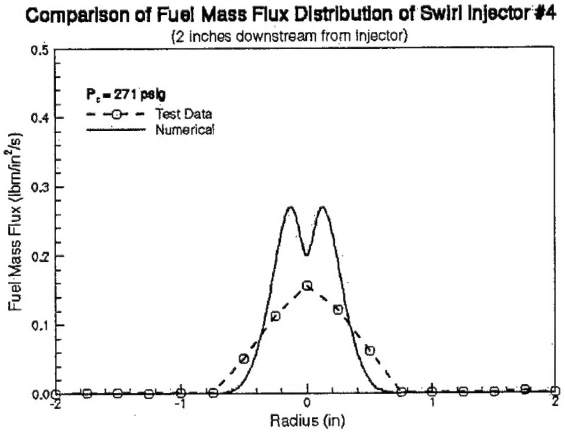

Figure 9. Averaged Mass Flux of Fuel at 2 in. Downstream from the Injector

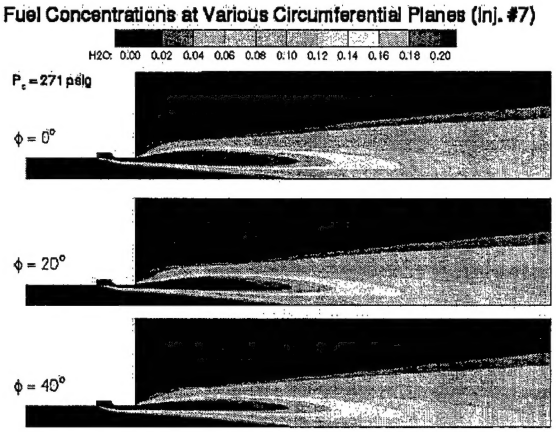

Figure 10. Mass Fraction Contours of Fuel at Various Circumferential Planes (Injector #7)

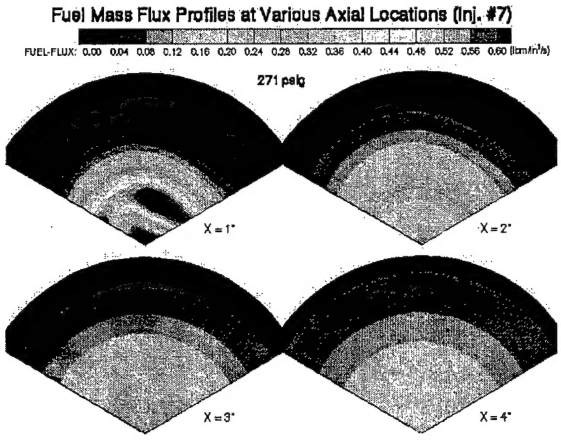

Figure 11. Fuel Mass Flux Contours at Various Axial Locations

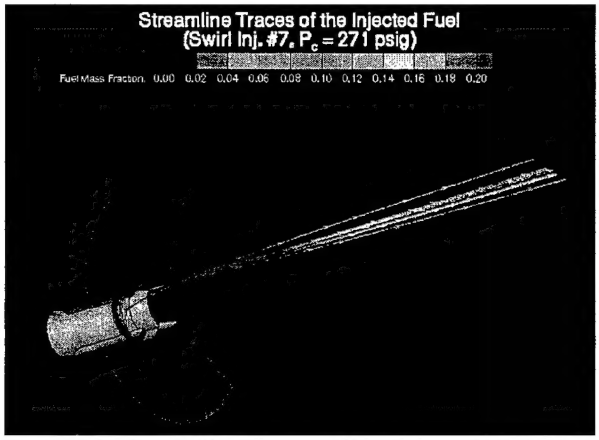

Figure 12. Streamline Traces of the Injected Fuel

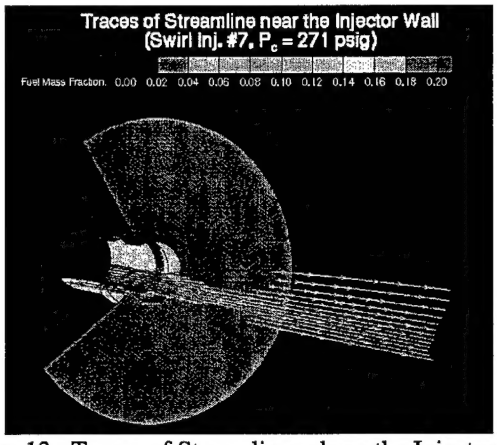

Figure 13. Traces of Streamlines along the Injector Wall

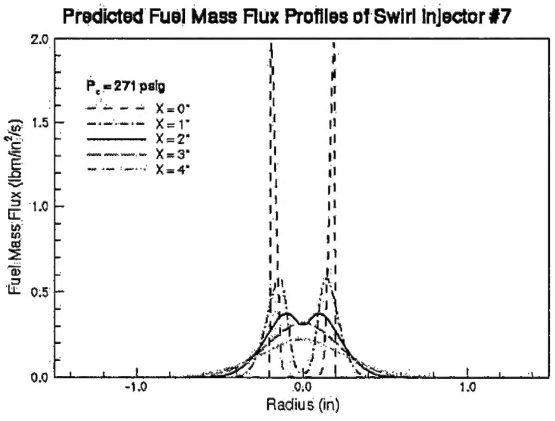

Figure 14. Averaged Mass Flux of Fuel at Various Axial Locations

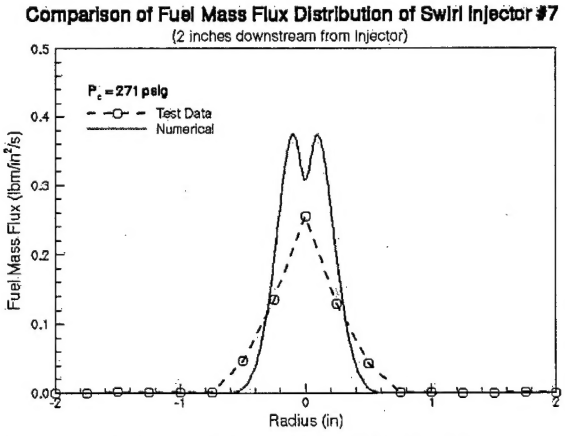

Figure 15. Averaged Mass Flux of Fuel at 2 in. Downstream from the Injector

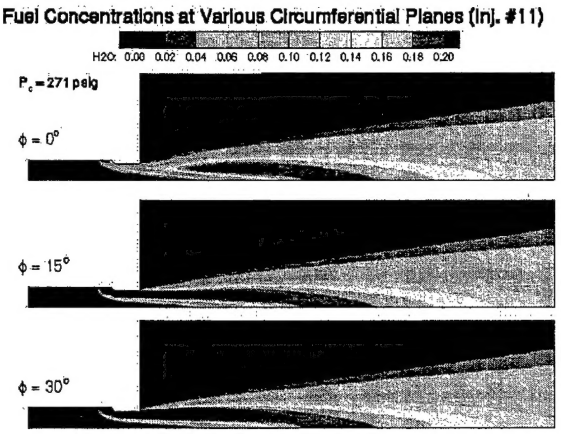

Figure 16. Mass Fraction Contours of Fuel at Various Circumferential Planes (Injector #11)

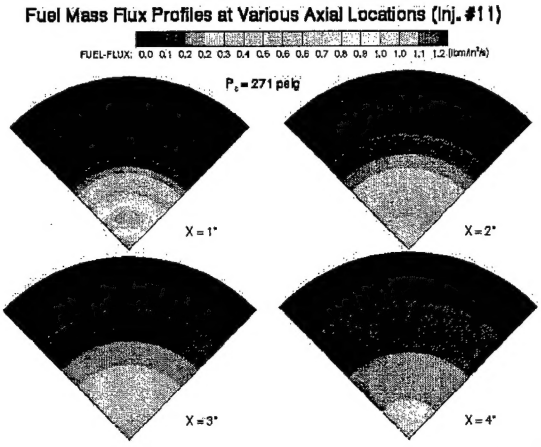

Figure 17. Fuel Mass Flux Contours at Various Axial Locations

Figure 18. Streamline Traces of the Injected Fuel

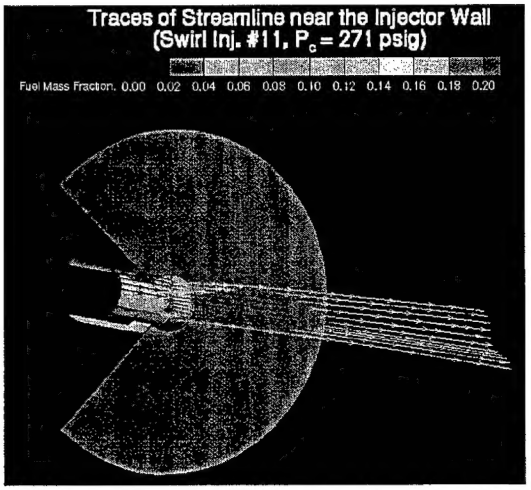

Figure 19. Traces of Streamlines along the Injector Wall

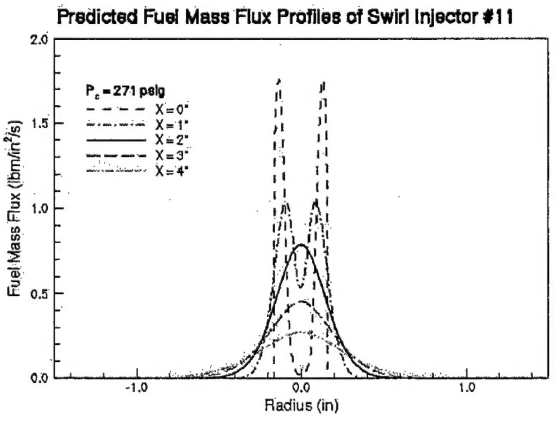

Figure 20. Averaged Mass Flux of Fuel at Various Axial Locations

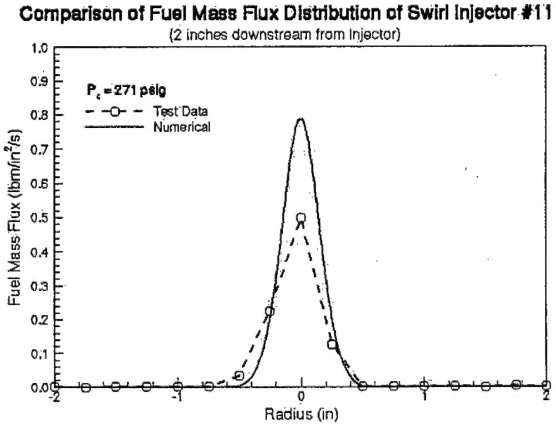

Figure 21. Averaged Mass Flux of Fuel at 2 in. Downstream from the Injector

DISCUSSION

Comparison of the CFD analysis results to the test data shows that the model picks up the major flow phenomena and trends as measured in the cold flow tests. Figure 22 illustrates that the analysis predicts the same order of peak water mass flux as measured in the cold flow experiments for the 3 injectors (injectors #4, #7, and #11). The relative differences in peak mass flux are well predicted by the model. Additionally, the spray fan angle also appears to be matched between the model and the experiments.

One striking difference between the computational and experimental results it the presence of the lobed structure in injectors 4 and 7 in the computations but were not seen in the experiments. This is likely caused by a combination of two effects. First, due to lack of spatial resolution of the measured mass-flux data, it is impossible to determine if the lobed structure predicted for injectors 4 and 7 is present in the cold flow experiment. Second, integration of the cold flow fuel flux results for injectors 4 and 7 greatly under-estimate total water flow. This suggests that a structure may have occurred, but may have been missed by the patternator. The stagnation region present along the centerline of the chamber will tend to cause this effect as the droplets, particularly the smaller droplets, will not be able to enter the measurement tubes. It is also likely that these droplets reflect off of the stagnation region and are measured in tubes farther from the centerline. This could explain the loss of this feature as well as the additional width of the experimental profiles. In contrast, integration of the cold flow fuel flux for injector 11 shows a smaller under-estimation, indicating the lobed structure may not have occurred during testing of this element as indicated by the CFD analysis. It is possible that the acceleration generated in the converging section of this injector gave the fluid droplets sufficient momentum to pierce the stagnation bubble.

Some simplifying assumptions with in the CFD model may cause error in the numerical analysis. One possible cause of error in the analysis is the homogenous spray model employed by the FDNS-RFV code, where the propellant mixing is predicted by the turbulence model which was tuned based on the incompressible flows. All operating chamber pressures are much lower than the critical pressure of water, and the flowfield is subjected to the subcritical spray condition where the inter-phase effects such as droplet atomization, droplet/turbulence interaction, and momentum lag, are very important. The homogeneous spray model, which assumes the particulate phase and the gas phase to be in equilibrium (i.e. no lag in momentum and heat transfer), is suitable for spray at the supercritical or near the critical condition, thus it could under-predict the propellant mixing in the case of sub-critical water. It should be noted that liquid rocket engines operate at high supercritical condition. The water/GN_2 injector cold flow test may not resemble the injector flow in real rocket engines. However, as previously described, the sub-critical results for mixing are likely conservative, i.e., supercritical conditions will tend to enhance the amount of mixed fluid due to the greater shear layer growth rates and a lack of a latent heat of vaporization. The favorable comparison of mixing trends between the CFD analysis and the cold flow tests provides confidence that the CFD analysis can be an effective tool in injector design to both predict cold flow and, potentially, hot fire data. When comparing the results, one must be careful to account for the differences resulting from the subcritical and supercritical behaviors of fluids.

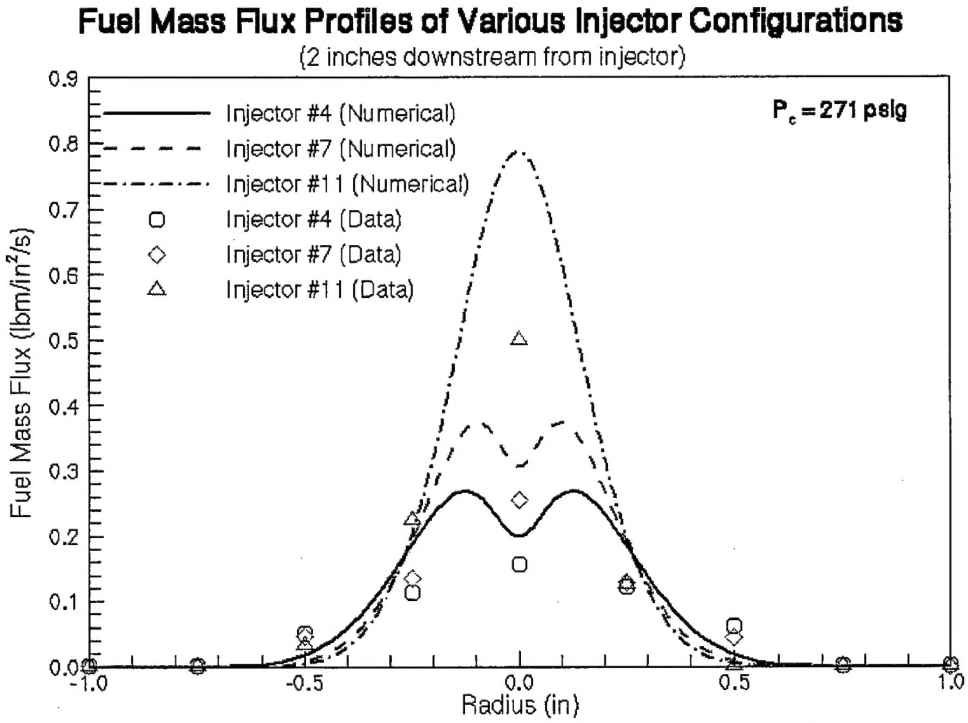

Figure 22. Averaged Fuel Mass Flux Profiles of Various Injector Configurations

EFFECTS OF GEOMETRY

The contour and stream profiles demonstrate the physics behind the mixing in these elements. The swirling fuel creates an annulus of fuel on the inner wall of the bottom portion of the GOX post. The GOX stream through the post shears that annulus into a cylindrical sheet of fuel, which cools the wall. The centrifugal force pushes the fuel towards the wall. At the same time, the reduced static pressure of the GOX stream (due to its substantial velocity) causes a pressure gradient which opposes the centrifugal head caused by the swirl. Consequently, the amount of mixing which occurs in the post is a function of the swirl rate and the GOX velocity. As the fuel leaves the post, the sheet breaks into "droplets" and tends to be pushed away from the center flow. As the fuel travels away from the injector face, the fuel gets entrained into the GOX flow.

From the above description of injector operation, it can be deduced that geometry plays an important role in mixing efficiency. For example, a smaller GOX post diameter creates faster GOX velocity, thereby increasing entrainment (as can be seen from injector #11). This helps explain why injector #4 does not mix as well as the others; the GOX velocity is slowed through the post as it diverges. Future results hope to separate out these two effects to examine the relative importance of each. It should be noted that slowing the swirl will reduce the fuel sheet that reaches the end of the post. That sheet is important for the prevention of burning the injector tip.

Though optimized mixing efficiency is the goal of the injector design, the rapid mixing may raise an issue of injector burn out under the hot fire condition. Moreover, differences between the hot fire and cold flow conditions are expected. Experimental and numerical investigations of the hot flow environment of the swirl injectors are needed to optimize the mixing efficiency and ensure hardware integrity.

EFFECTS OF CHAMBER PRESSURE

To study the effect of chamber pressure on mixing efficiency, Injector #11 was studied at chamber pressures of 271 psig and 842 psig. The averaged fuel mass flux profiles plotted in Figures 23. Both the test data and the analysis indicate that chamber pressure does not have a strong effect on the mass distribution profile, indicating consistency between the analysis and the cold flow tests. These results also suggest that this injector element should perform well under throttled conditions. Note that the mass flow was increased to emulate the higher flows required to increase chamber pressure and a real combustor.

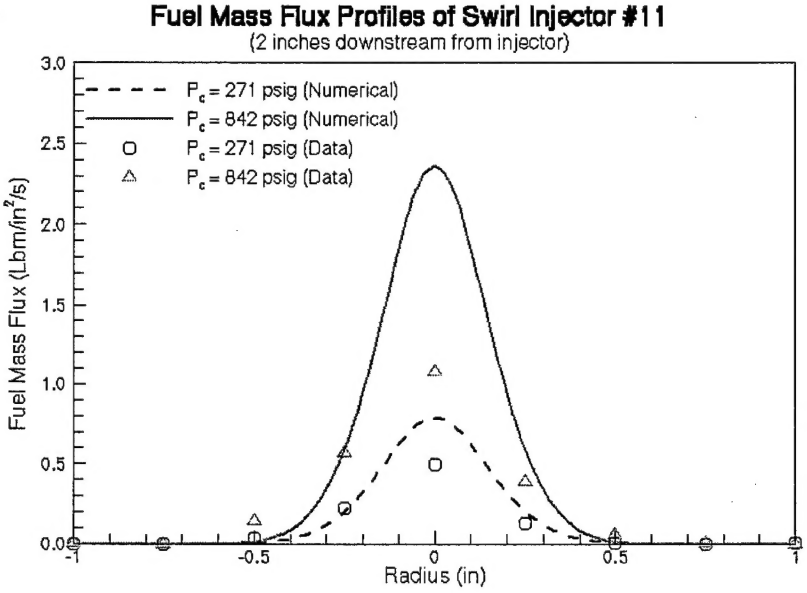

Figure 23. Averaged Fuel Mass Flux Profiles of Injector #11 with Different Pressures

CONCLUSION

Comparison of the cold flow measurements to the CFD analysis suggests that FDNS is capable of determining major trends in mixing phenomenon for this swirl coaxial element and consequently the CFD analysis can aid in design of the injector. Specifically, the analysis predicts the same order of peak water mass flux as measured in the cold flow experiments for different injector geometry configurations. The analysis predicts the solid cone spray distribution consistently measured during the cold flow tests.

FDNS' homogeneous spray model is not well suited for the cold flow analysis since the model assumes the inter-phase effect (surface tension) to be negligible in a supercritical mixture. When using water below its critical pressure, the assumption of supercritical fluid in phase equilibrium was not met. However, the results show that the homogeneous spray model is sufficient to make relative comparisons between different injectors. The model is expected to be more accurate for the supercritical conditions existing in the real combustion process.

The model shows the physical phenomena causing the mixing in these elements. The elements swirl the fuel around the inside of the GOX post. That fuel is swept out of the GOX post in a sheet and then entrained into the high velocity GOX flow downstream of the element.

Insufficient simulations were completed to determine the sensitivity of the mixing to major parameters such as GOX velocity, fuel swirl, and injector geometry, but the simulations completed suggest that the models are capable of providing meaningful results for these types of parametric studies.

FUTURE WORK

To better understand the physics of the swirl coaxial element, a parametric CFD study will be completed in which GOX velocity, fuel swirl, and chamber pressure are varied to determine the effects on injector performance. The same parametric study should be completed with cold flow tests to compare trends.

Finally, several analyses have been completed for hot fire operation. These results should be compared to the uni-element hot fire testing that is currently in progress at AFRL, and then validated. If the analyses appear reasonable, they should be used to help prevent unacceptable face heating loads on the injector.

REFERENCES

1. Muss, J.A., Johnson, C.W., Cohn, R., Strakey, P.A., Bates, R. W., Talley, D.G. "Swirl Coaxial Injector Development Part I, Test and Results" JANNAF Combustion Subcommittee, April 8-11, 2002, Destin FL.
2. Cheng, G.C. and Farmer, R.C., "CFD Spray Combustion Model for Liquid Rocket Engine Injector Analyses," AIAA Paper 2002-0785.
3. Cheng, G.C., Anderson, P.G., and Farmer, R.C., "Development of CFD Model for Simulating Gas/Liquid Injectors in Rocket Engine Design," AIAA Paper 97-3228, 1997.
4. Farmer, R.C., Cheng, G.C., Trinh, H., and Tucker, K., "A design Tool for Liquid Rocket Engine Injectors," AIAA 2000-3499, 2000.
5. Chen, Y.S., "Compressible and Incompressible Flow Computations with a Pressure Based Method," AIAA Paper 89-0286, 1989.
6. Hirschfelder, J.O., et al, "Generalized Equations of State for Gases and Liquids," IEC, 50, pp.375-385, 1958.
7. Hirschfelder, J.O., et al, "Generalized Excess Functions for Gases and Liquids," IEC, 50, pp.386-390, 1958.
8. Reid, R.C., et al, The Properties of Gases & Liquids, 4th ed., McGraw-Hill, 1987.
9. Gordon, S., and B.J. McBride, "Computer Program for Calculation of Complex Chemical Equilibrium Compositions, Rocket Performance, Incident and Reflected Shocks, and Chapman-Jouget Detonations," NASA-SP-273, 1971.
10. Saad, Y., and Schultz, M.H., SIAM Journal of Sci. Stat. Comput., Vol. 7, pp. 856-869, 1986.
11. Chehroudi, B., Talley, D.G., and Coy, E.; "Visual Characteristics and Initial Growth Rates of Round Cryogenic Jets at Subcritical and Supercritical Pressures," *Physics of Fluids*, Vol. 14, No. 2, 2002.